Climatic Change
DOI 10.1007/s10584-014-1217-x

LETTER

Satellite-based rainfall data reveal a recent drying trend in central equatorial Africa

Jeremy E. Diem · Sadie J. Ryan · Joel Hartter · Michael W. Palace

Received: 14 January 2014 / Accepted: 16 July 2014

Abstract West-central Uganda, a biodiversity hotspot on the eastern edge of central equatorial Africa (CEA), is a region coping with balancing food security needs of a rapidly growing human population dependent on subsistence agriculture with the conservation of critically endangered species. Documenting and understanding rainfall trends is thus of critical importance in west-central Uganda, but sparse information exists on rainfall trends in CEA during the past several decades. The recently created African Rainfall Climatology version 2 (ARC2) dataset has been shown to perform satisfactorily at identifying rainfall days and estimating seasonal rainfall totals in west-central Uganda. Therefore, we use ARC2 data to assess rainfall trends in west-central Uganda and other parts of equatorial Africa from 1983–2012. The core variables examined were three-month rainfall variables for west-central Uganda, and annual rainfall variables and seasonal rainfall totals for a transect that extended from northwestern Democratic Republic of the Congo to southern Somalia. Significant decreases in rainfall in west-central Uganda occurred for multiple three-month periods centered on boreal summer, and rainfall associated with the two growing seasons decreased by 20 % from 1983–2012. The drying trend in west-central Uganda extended westward into the Congo rainforest. Rainfall in CEA was significantly correlated with the Atlantic Multidecadal Oscillation (AMO) at the annual scale and during boreal summer and autumn. Two other possible causes of the decreasing rainfall in CEA besides North Atlantic Ocean sea-surface temperatures (e.g.,

J. E. Diem (✉)
Department of Geosciences, Georgia State University, P. O. Box 4105, Atlanta, GA 30302, USA
e-mail: jdiem@gsu.edu

S. J. Ryan
Department of Geography, University of Florida, Gainesville, FL 32611, USA

S. J. Ryan
Emerging Pathogens Institute, University of Florida, Gainesville, FL 32611, USA

J. Hartter
Environmental Studies Program, University of Colorado, UCB 397, Boulder, CO 80309, USA

M. W. Palace
Earth Systems Research Center, Institute for the Study of Earth, Oceans, and Space, University of New Hampshire, Durham NH 03824, USA

Published online: 22 August 2014

AMO), are the warming of the Indian Ocean and increasing concentrations of carbonaceous aerosols over tropical Africa from biomass burning.

1 Introduction

Virtually no reliable information exists on trends in rainfall in central equatorial Africa (CEA) over the past several decades, due to sparse and interrupted ground measurements. The CEA region extends from the Republic of the Congo (~15° E) to western Uganda (~32° E) (Todd and Washington 2004) (Fig. 1a). Trenberth et al. (2007) show that insufficient data exists for most – if not all – of CEA to determine annual rainfall trends from 1979–2005. Washington et al. (2013) report a dramatic decline in the number of rain gauges in the Democratic Republic of the Congo (DRC) from 1980 to 2010, with just three meteorological stations reporting to the Global Telecommunication System in 2013. Rainfall records in Uganda also are scant, and most existing ones were interrupted for long periods in the 1970s and 1980s due to political turmoil (Kizza et al. 2009).

The intra-annual variability in CEA rainfall is controlled strongly by the north–south movement of the Intertropical Convergence Zone (ITCZ) and the associated rainbelt (Nicholson and Grist 2003; Jackson et al. 2009). Mesoscale convective complexes, rather than local convective storms, are responsible for much of the rainfall in the region (Jackson et al. 2009). Mean rainfall averaged over CEA peaks in the transition months of October-November and March-May, and the annual rainfall total is approximately 1,500 mm (Todd and

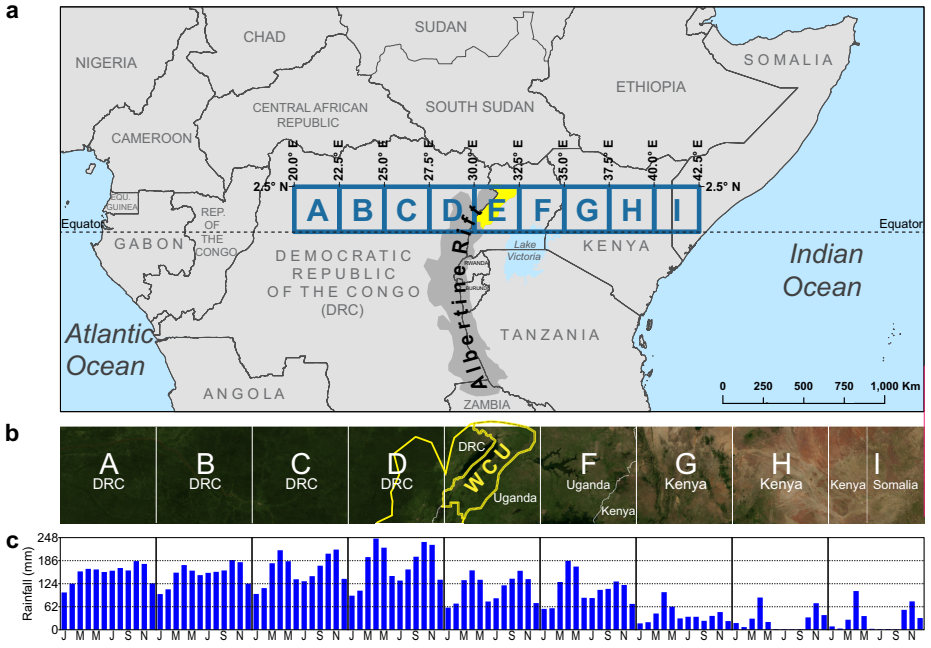

Fig. 1 **a** Geographical location of west-central Uganda (WCU) in tropical Africa at the northern end of the Albertine Rift and the transect of nine 2.5° cells extending from northwestern Democratic Republic of the Congo to southern Somalia. WCU (in yellow) is located almost entirely within cell E. **b** True-color April image of a portion of equatorial Africa obtained from the National Aeronautics and Space Administration's Blue Marble Next Generation dataset. The yellow polygon is the boundary of the Albertine Rift. **c** Mean monthly rainfall totals for the nine cells during 1998–2012 from the Africa Rainfall Climatology Version 2 (ARC2) product

Washington 2004). Equatorial DRC (i.e., the Congo rainforest) receives more than 1,800 mm yr^{-1} (Liebmann et al. 2012) and does not have a true dry season (Herrmann and Mohr 2011) (Fig. 1b,c). Finally, the interannual variability of rainfall totals in CEA is complex: the factors governing the interannual variability are season-specific and include Atlantic, Indian, and Pacific sea-surface temperatures (Balas et al. 2007).

West-central Uganda, home to some of the world's most rapidly growing human populations (Population Reference Bureau 2013), lies on the eastern edge of CEA in the far northeastern portion of the Albertine Rift, which is one of the world's hotspots for biodiversity (Cordeiro et al. 2007; Plumptre et al. 2007) (Fig. 1). The vast majority of households in west-central Uganda practice rain-fed subsistence agriculture, where planting and harvesting cycles are timed with the rainy season allowing for crops to ripe (Hartter et al. 2012). The dependence of the increasing rural populations in west-central Uganda, and in the Albertine Rift as a whole, on subsistence agriculture has caused much land and resource pressure and high rates of habitat loss and conversion (Brooks et al. 2001; Fisher and Christopher 2007). The often conflicting needs for conservation in this biodiversity hotspot and food security for millions of people in this region proves critical in the need to understand regional rainfall trends.

The purpose of this study is to assess rainfall trends in CEA from 1983–2012 using a newly created dataset, African Rainfall Climatology version 2 (ARC2). ARC2 is a high-resolution, satellite-based precipitation dataset that uses two uniform inputs, calibrated infrared satellite imagery and quality-controlled gauge observations, to produce daily rainfall estimates; consequently, it is expected to be homogeneous over time and be useful for assessing rainfall trends (Novella and Thiaw 2013). ARC2 performs satisfactorily at identifying rainfall days and estimating seasonal – and presumably annual – rainfall totals in areas of west-central Uganda that are not in rainshadows or dominated by the warm orographic rain process (Diem et al. in press). The main deficiencies of ARC2 are underestimating the following: boreal-summer rainfall totals, high rainfall totals, and rainfall over complex topography (Novella and Thiaw 2013). While ARC2 captures the interannual variability in rainfall totals well (Novella and Thiaw 2013), it is important to note that the capability of ARC2 to accurately assess rainfall trends in CEA and other regions is unknown at present.

2 Data and methods

2.1 Daily rainfall estimates

Daily ARC2 data were acquired from the International Research Institute for Climate and Society at Columbia University for cells A-I and west-central Uganda (Fig. 1a-c). The data, which have a spatial resolution of 0.10°, were obtained for 1983–2012, and the dataset was missing rainfall totals for 340 out of 10,958 days. ARC2 are developed by the Climate Prediction Center of the National Oceanic and Atmospheric Administration for the Famine Early Warning Systems Network (FEWS NET).

2.2 Three-month analyses for west-central Uganda

Totals for rainfall, rainfall days, first-quartile rainfall days, and fourth-quartile rainfall days were calculated for each overlapping three-month period (e.g., November-January, December-February, etc.) for west-central Uganda for each of the thirty years. West-central Uganda contained 326 ARC2 cells, the minimum rainfall total for a rainfall day was 0.2 mm, and the

quartile thresholds were specific to each of the three-month periods. If a three-month period was missing more than 10 % of the daily values, then it was not given a rainfall value. The remaining periods had rainfall totals upwardly adjusted using the ratio of total days per period by the number of days with a valid rainfall total.

2.3 Seasonal and annual analyses for transect cells

Seasonal [(December-February (DJF), March-May (MAM), June-August (JJA), and September-November (SON)] totals of rainfall along with annual totals of rainfall, rainfall days, first-quartile rainfall days, and fourth-quartile rainfall days were calculated for each of the nine 2.5° cells (i.e., A-I) (Fig. 1). Each cell contained 676 ARC2 cells. The procedure described in section 2.2 for eliminating and upwardly adjusting values was used for the transect cells.

2.4 Multi-decadal trends

All trends in rainfall variables were assessed using one-tailed Kendall-Tau correlation tests with a significance level of 0.01. The Kendall-Theil robust line was used to estimate changes from 1983–2012; this method is affected minimally by outliers, since it estimates slope by calculating the median of the slopes between all combinations of two points in the data (Helsel and Hirsch 2002).

2.5 Connections to climate-variability indices

Correlations between rainfall totals and climate-variability indices were calculated to better understand the connections between large-scale tropical circulation and rainfall across the transect. One-tailed Pearson product–moment correlation tests were used to identify significant (α=0.01) correlations between the rainfall totals and three indices: the Atlantic Multidecadal Oscillation (AMO), the Dipole Mode Index (DMI), and the Niño 3.4 index. The AMO is an index of sea-surface temperatures (SSTs) centered on the North Atlantic Ocean (Knight et al. 2005). The negative phase of the AMO has been linked to the occurrence of Sahel drought (Knight et al. 2006), and the AMO is negatively correlated with boreal-summer rainfall in the western and central parts of equatorial Africa (Knight et al. 2006; Zhang and Delworth 2006). The DMI is derived from differences in SST from the tropical western Indian Ocean (50° E – 70° E, 10° S – 10° N) and the tropical southeastern Indian Ocean (90° E – 110° E, 10° S – Equator) (Saji et al. 1999); it is a measure of the Indian Ocean Dipole (IOD). Large DMI values are associated with heavy boreal-autumn rainfall in East Africa (Black et al. 2003; Behera et al. 2005). Niño 3.4 is an SST index for the central equatorial Pacific Ocean (5°N–5°S, 120°–170°W); large positive (negative) values indicate El Niño (La Niña) events (Trenberth 1997). Strong ENSO (El Niño/Southern Oscillation) signals exist in eastern equatorial Africa (EEA): boreal-autumn rainfall is enhanced during El Niño events (Nicholson and Kim 1997). The Niño 3.4 index may not be as important as the DMI as a control of rainfall in eastern tropical Africa: the correlation between ENSO and boreal-autumn rainfall in parts of East Africa is insignificant when the IOD is removed (Behera et al. 2005). Monthly AMO data, calculated from the Kaplan SST version 2 data, and Niño 3.4 data, calculated from the NOAA OI SST version 2 data, were obtained from the National Oceanic and Atmospheric Administration. Monthly DMI data, calculated from HadISST data, were obtained from the Japan Agency for Marine-Earth Science and Technology.

3 Results

3.1 West-central Uganda

West-central Uganda has an annual rainfall total of approximately 1,200 mm, with the two rainy seasons (i.e., first rains and second rains) occurring during March-June and from July-November (Fig. 1c). The wettest and driest three-month periods are August-October (430 mm) and December-February (170 mm), respectively.

There were significant trends in three-month rainfall values in west-central Uganda from 1983–2012 (Fig. 2). Rainfall decreased significantly during April-June, June-August, and October-December (Fig. 2a). There was a 20 % decrease in rainfall from 1983–2012 during three-month periods associated with the two growing seasons (i.e., the rainy seasons). Rainfall-day frequencies increased during all three-month periods, but only the trend for August-October was significant (Fig. 2b). Rainfall intensity decreased and the frequency of light-rainfall days increased during each period, with only November-January not having significant trends (Fig. 2c,d). Each three-month period also had decreasing trends in the frequency of heavy-rainfall days, and the significant trends existed from boreal spring to boreal autumn (Fig. 2e).

Rainfall in west-central Uganda is connected more closely to the AMO than the DMI and Niño 3.4 index (Fig. 2f). The only significant correlations were significant negative correlations between April-June, June-August, and August-October rainfall and the AMO. The DMI and Niño 3.4 index had the largest correlations with rainfall during the boreal-winter periods.

3.2 Nine-cell transect

Annual rainfall totals decreased substantially from west to east across the nine-cell transect (Fig. 1c). The Congo rainforest cells (A-D) received 1,700 to 1,800 mm of rainfall annually,

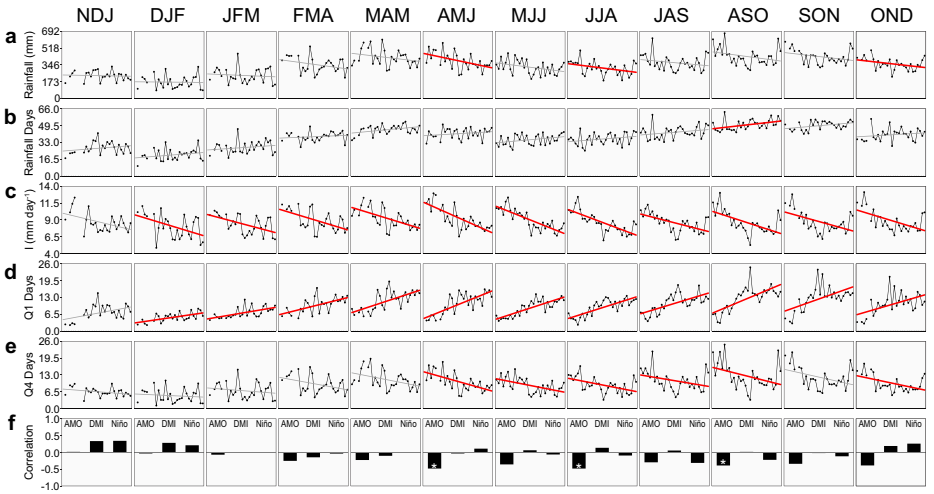

Fig. 2 Time series from 1983–2012 of **a** rainfall totals, **b** rainfall days, **c** rainfall intensity (I) for rainfall days, **d** first-quartile (Q1) rainfall days, and **e** fourth-quartile (Q4) rainfall days. **f** correlations from 1983–2012 between seasonal rainfall totals and the Atlantic Multidecal Oscillation (AMO), the Dipole Mode Index (DMI), and the Niño 3.4 index; asterisks indicate significant (α=0.01; one-tailed) correlations

the Uganda cells (E and F) received 1,200 to 1,300 mm of rainfall, and the EEA cells (G-I) received 300 to 700 mm of rainfall. The wettest seasons for the Congo rainforest and Uganda cells were MAM and SON, while the wettest season for the EEA cells was MAM, which is known as the long rains in the region. The driest season for the Congo rainforest and Uganda cells was DJF, while the driest season for the EEA cells was JJA.

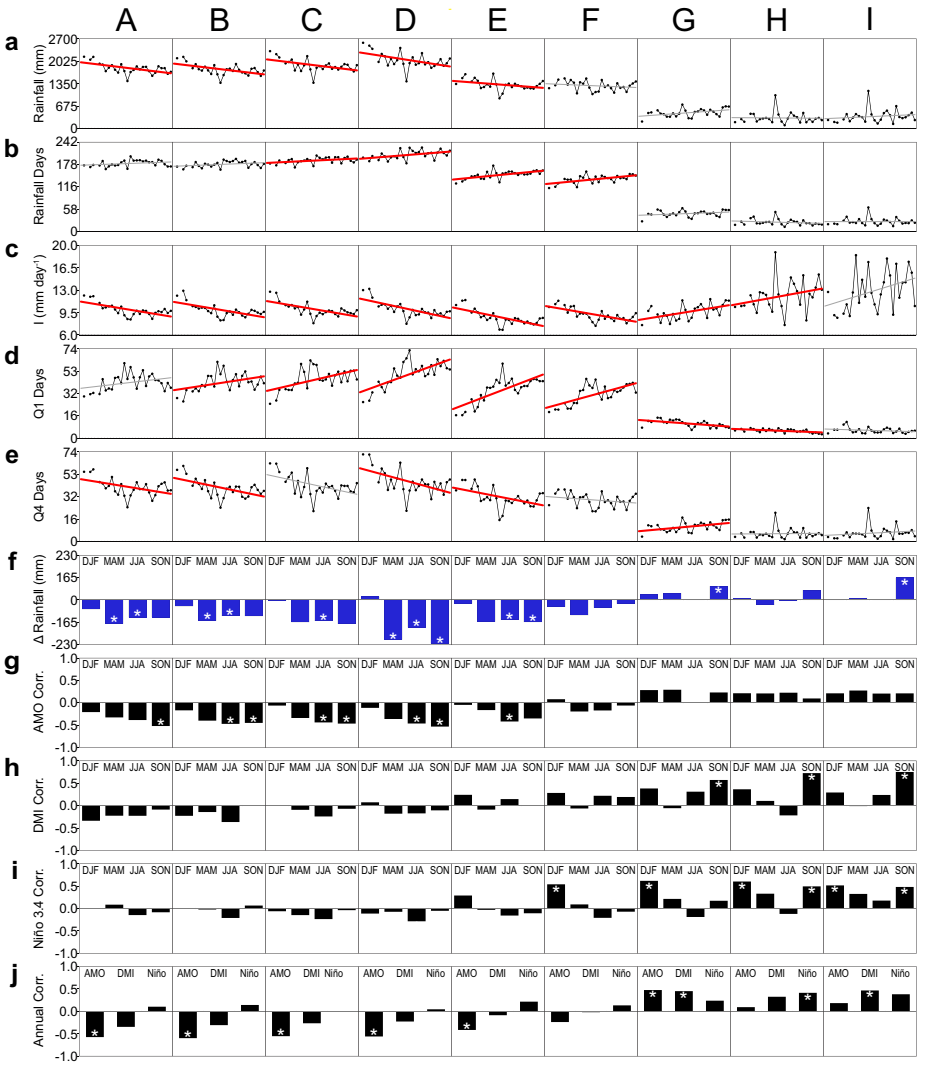

Fig. 3 Time series from 1983–2012 for cells A-I (see Fig. 1) of **a** annual rainfall, **b** rainfall days, **c** intensity (I) of rainfall days, **d** first-quartile (Q1) rainfall days, and **e** fourth-quartile (Q4) rainfall days. Red lines indicate significant (α=0.01; one-tailed) trends in annual values and grey lines indicate non-significant trends. **f** Difference from 1983 to 2012 in seasonal rainfall totals; asterisks indicate significant (α=0.01; one-tailed) trends in seasonal rainfall. Correlations from 1983–2012 between seasonal rainfall totals and g the Atlantic Multidecal Oscillation, **h** the Dipole Mode Index, and **i** the Niño 3.4 Index; asterisks indicate significant (α=0.01; one-tailed) correlations. **j** Correlations between annual rainfall totals and AMO, DMI, and Niño 3.4

The drying trend in west-central Uganda from 1983–2012 extended westward into the Congo rainforest and was nonexistent eastward in Kenya and southern Somalia (Fig. 3). Cells A-E experienced significant decreases in annual rainfall, while cells F-I did not experience a significant change in annual rainfall (Fig. 3a). Significant decreases in rainfall intensity and increases in light-rainfall days occurred at cells B-F, while significant increases in rainfall intensity and decreases in light-rainfall days occurred at cells G and H (Fig. 3c,d). Most of the western cells had significant decreases in heavy-rainfall days, while cell G had a significant increase in heavy-rainfall days (Fig. 3e). Significant seasonal decreases in rainfall occurred for cells A-E during either MAM, JJA, or SON seasons, with all five cells having significant decreases during JJA. Cells G and I had significant increases in SON (i.e., short rains) rainfall (Fig. 3f).

Rainfall in the western cells was significantly correlated with the AMO, while rainfall in the eastern cells was significantly correlated with the DMI and Niño 3.4 index (Fig. 3g-j). Similar to what was found for west-central Uganda, there were significant negative correlations between JJA and SON rainfall in the western cells and the AMO (Fig. 3g). Significant positive correlations between seasonal rainfall at the eastern cells and the DMI and Nino 3.4 were as follows: SON rainfall and the DMI; DJF rainfall and Niño 3.4; and SON rainfall and Niño 3.4. Annual rainfall in CEA was significantly negatively correlated with the AMO, while annual rainfall in EEA was significantly positively correlated with the DMI and Niño 3.4. Cell F (i.e., eastern Uganda) was the only cell without significant annual correlations.

4 Discussion

Rainfall trends and correlations with large-scale tropical circulation vary markedly between CEA and EEA. CEA rainfall, which decreased significantly from 1983–2012, is highly correlated with the AMO, while EEA rainfall during the short-rains season, which increased significantly, is highly correlated with the DMI and Niño 3.4 index. Uganda as a whole is neither in CEA or EEA: west-central Uganda is on the eastern edge of CEA, while eastern Uganda, in which rainfall is poorly correlated with climate-variability indices, is a transition zone between CEA and EEA. The results in this paper for the long rains season in EEA differ slightly from findings by Williams and Funk (2011), using datasets other than ARC2. We report only a small decrease in rainfall in eastern Kenya during MAM, while Williams and Funk (2011), report large decreases in March-June rainfall in eastern Kenya from 1980–2009.

North Atlantic Ocean SSTs appear to have played a role in the decreasing rainfall in CEA from 1983–2012. The ITCZ in the Atlantic sector shifts northward during a warm phase AMO (Knight et al. 2006; Zhang and Delworth 2006; Ting et al. 2011). Over the past several decades, the AMO was at its most negative value (i.e., peak of the cold phase) in the late 1970s and transitioned to the warm phase in the 1990s (see Knight et al. 2005). The significant negative correlations between the AMO and rainfall during boreal summer and autumn in the CEA support the northward shift of the Atlantic ITCZ as a cause of the decreasing rainfall in CEA. Other studies (Zhang and Delworth 2006; Balas et al. 2007) also have indicated that North Atlantic Ocean SSTs are negatively correlated with boreal-summer rainfall in CEA.

Although correlations between CEA rainfall and the DMI were not significant, Indian Ocean SSTs cannot be eliminated as a contributor to the declining CEA rainfall. The Indian Ocean has warmed relatively rapidly over the past several decades, and the warm pool of the Indian Ocean has expanded approximately 40° westward (Williams and Funk 2011). The DMI also has displayed an upward trend over the past several decades (Cai et al. 2013). A modeled warming of the equatorial/tropical Indian Ocean for February-April and July-September has been shown

to affect the Africa/Indian Ocean Walker cell, whereby large-scale subsidence and reduced rainfall would occur over CEA and increased rainfall would occur over EEA (Hoerling et al. 2006; Mohino et al. 2011). Other simulations show a weakening of the Walker circulation with increasing greenhouse-gas concentrations; as a result, middle-troposphere subsidence increases over CEA and decreases over EEA (Vecchi and Soden 2007; Shongwe et al. 2011). Williams and Funk (2011), who report decreasing rainfall during the long rains in EEA from 1980–2009, note that over the past several decades during March-June there has been a westward extension of the ascending branch of the tropical Walker circulation, rather than a weakening of the Walker circulation, that has likely led to increased vertical ascent across the southern tropical Indian Ocean and accompanying decreased ascent and decreased rainfall over eastern Africa.

Increasing concentrations of carbonaceous aerosols also may have contributed to the drying trend in CEA. Biomass burning in tropical Africa has led to some of the highest concentrations of carbonaceous aerosols (i.e., black carbon and particulate organic matter) in the world over CEA (Stier et al. 2005; Paeth and Fichter 2006). The high concentrations over CEA are the result primarily of aerosols transported to the equator from landscape fires northward and southward of the Congo rainforest (Roberts et al. 2009). The effects of aerosols on clouds mostly act to suppress precipitation, through increased atmospheric stability and the large numbers of small cloud droplets inhibits the two leading precipitation formation processes (Nober et al. 2003; Rosenfeld et al. 2008). Therefore, the aerosols may be responsible for a paradoxical situation: CEA has the highest lightning frequency in the world but relatively low rainfall totals compared to other equatorial regions (Nicholson and Grist 2003; Jackson et al. 2009). Modeling studies suggest increased aerosol concentrations over tropical Africa (Paeth and Fichter 2006; Kawase et al. 2011; Tosca et al. 2013) should decrease rainfall in CEA. Increased aerosol concentrations should either directly or indirectly cause subsidence over tropical Africa, and, in turn, suppress rainfall in CEA (Paeth and Fichter 2006; Kawase et al. 2011; Tosca et al. 2013). For example, Tosca et al. (2013) focus on carbonaceous-aerosol emissions from landscape fires globally, and moving from scenario with no landscape fires to a scenario with the present-day magnitude of landscape fires results in CEA having the largest rainfall decreases globally, and the rainfall decreases do not extend into EEA.

5 Conclusions

Parts of CEA may be in a precarious position in terms of food security owing to an increase in population, land shortages, and – as our results show from an examination of ARC2 data – a decrease in rainfall. Declining rainfall in CEA from 1983–2012 was centered on boreal summer, and rainfall in west-central Uganda – which represents the far eastern portion of CEA – decreased by 20 % during both growing seasons. These changes will almost certainly have negatively impacted food security in west-central Uganda. Three possible causes of the decreasing rainfall in CEA are a northward shift of the ITCZ associated with the AMO, a weakening of or westward shift or both of the Africa/Indian Ocean Walker cell linked to a warming of the Indian Ocean and increasing global temperatures, and increasing concentrations of carbonaceous aerosols over tropical Africa from biomass burning. Future research is needed to further verify the drying trend in CEA using additional climate datasets proven to accurately estimate seasonal rainfall totals in the region.

Acknowledgments This research was supported by a National Science Foundation Coupled Natural-Human Systems Exploratory grant (NSF-EX: 1114977). We are grateful to the three anonymous reviewers for their comments that greatly improved the article.

References

Balas N, Nicholson SE, Klotter D (2007) The relationship of rainfall variability in West Central Africa to sea-surface temperature fluctuations. Int J Clim 27:1335–1349

Behera SK, Luo J-J, Masson S, Delecluse P, Gualdi S, Navarra A, Yamagata T (2005) Paramount impact of the Indian Ocean Dipole on the East African short rains: a CGCM study. J Clim 18:4514–4530

Black E, Slingo J, Sperber KR (2003) An observational study of the relationship between excessively strong short rains in coastal East Africa and Indian Ocean SST. Mon Weather Rev 131:74–94

Brooks T, Balmford A, Burgess N, Fjeldsa J, Hansen LA, Moore J, Rahbek C, Williams P (2001) Toward a blueprint for conservation in Africa. Bioscience 51:613–624

Cai W, Zheng X-T, Weller E, Collins M, Cowan T, Lengaigne M, Yu W, Yamagata T (2013) Projected response of the Indian Ocean Dipole to greenhouse warming. Nat Geosci 6:999–1007

Cordeiro NJ, Burgess ND, Dovie DB, Kaplin BA, Plumptre AJ, Marrs R (2007) Conservation in areas of high population density in sub-Saharan Africa. Biol Cons 134:155–163

Diem JE. Hartter J. Ryan SJ. Palace MW (2014) Validation of satellite rainfall products for western Uganda. J Hydrometeor

Fisher B, Christopher T (2007) Poverty and biodiversity: measuring the overlap of human poverty and the biodiversity hotspots. Ecol Econ 62:93–101

Hartter J, Stampone MD, Ryan SJ, Kirner K, Chapman CA, Goldman A (2012) Patterns and perceptions of climate change in a biodiversity conservation hotspot. PLoS One 7:e32408

Helsel DR, Hirsch RM (2002) Statistical methods in water resources. In Hydrologic analysis and interpretation. U.S. Geological Survey, Washington, pp 1–510

Herrmann SM, Mohr KI (2011) A continental-scale classification of rainfall seasonality regimes in Africa based on gridded precipitation and land surface temperature products. J Appl Meteorol Climatol 50:2504–2513

Hoerling M, Hurrell J, Eischeid J, Phillips A (2006) Detection and attribution of twentieth-century northern and southern African rainfall change. J Clim 19:3989–4008

Jackson B, Nicholson SE, Klotter D (2009) Mesoscale convective systems over western equatorial Africa and their relationship to large-scale circulation. Mon Weather Rev 137:1272–1294

Kawase H. Takemura T. Nozawa T (2011) Impact of carbonaceous aerosols on precipitation in tropical Africa during the austral summer in the twentieth century. J Geophys Res 116:D18116

Kizza M, Rodhe A, Xu C-Y, Ntale HK, Halldin S (2009) Temporal rainfall variability in the Lake Victoria Basin in East Africa during the twentieth century. Theor Appl Climatol 98:119–135

Knight JR, Allan RJ, Folland CK, Vellinga M, Mann ME (2005) A signature of persistent natural thermohaline circulation cycles in observed climate. Geophys Res Lett 32, L20708

Knight JR, Folland CK, Scaife AA (2006) Climate impacts of the Atlantic Multidecadal Oscillation. Geophys Res Lett 33, L17706

Liebmann B, Bladé I, Kiladis GN, Leila MVC, Senay GB, Allured D, Leroux S, Funk C (2012) Seasonality of African precipitation from 1996 to 2009. J Clim 25:4304–4322

Mohino E, Janicot S, Bader J (2011) Sahel rainfall and decadal to multi-decadal sea surface temperature variability. Clim Dyn 37:419–440

Nicholson SE, Grist JP (2003) The seasonal evolution of the atmospheric circulation over West Africa and Equatorial Africa. J Clim 16:1013–1030

Nicholson SE, Kim J (1997) The relationship of the El Niño-Southern Oscillation to African rainfall. Int J Clim 17:117–135

Nober FJ, Graf H-F, Rosenfeld D (2003) Sensitivity of the global circulation to the suppression of precipitation by anthropogenic aerosols. Glob Planet Change 37:57–80

Novella NS, Thiaw WM (2013) African rainfall climatology version 2 for famine early warning systems. J Appl Meteorol Climatol 52:588–606

Paeth H, Fichter J (2006) Greenhouse-gas versus aerosol forcing and African climate response. Clim Dyn 26:35–54

Plumptre AJ, Davenport TRB, Behangana M, Kityo R, Eilu G, Ssegawa P, Ewango C, Meirte D, Kahindo C, Herremans M, Peterhans JK, Pilgrim JD, Wilson M, Languy M, Moyer D (2007) The biodiversity of the Albertine Rift. Biol Conserv 134:178–194

Population Reference Bureau (2013) World population data sheet. http://www.prb.org/Publications/Datasheets/2013/2013-world-population-data-sheet/data-sheet.aspx

Roberts G, Wooster MJ, Lagoudakis E (2009) Annual and diurnal African biomass burning temporal dynamics. Biogeosciences 6:849–866

Rosenfeld D, Lohmann U, Raga GB, O'Dowd CD, Kulmala M, Fuzzi S, Reissell A, Andreae MO (2008) Flood or drought: how do aerosols affect precipitation? Science 321:1309–1313

Saji NH, Goswami BN, Vinayachandran PN, Yamagata T (1999) A dipole mode in the tropical Indian Ocean. Nature 401:360–363

Shongwe ME, van Oldenborgh GJ, van den Hurk B, van Aalst M (2011) Projected changes in mean and extreme precipitation in Africa under global warming Part II: East Africa. J Clim 24:3718–3733
Stier P, Feichter J, Kinne S, Kloster S, Vignati E, Wilson J, Ganzeveld L, Tegen I, Werner M, Balkanski Y, Schulz M, Boucher O, Minikin A, Petzold A (2005) The aerosol-climate model ECHAM5-HAM. Atmos Chem Phys 5:1125–1156
Ting M, Kushnir Y, Seager R, Li C (2011) Robust features of Atlantic multi-decadal variability and its climate impacts. Geophys Res Lett 38, L17705
Todd MC, Washington R (2004) Climate variability in central equatorial Africa: influence from the Atlantic sector. Geophys Res Lett 31, L23202
Tosca MG, Randerson JT, Zender CS (2013) Global impact of smoke aerosols from landscape fires on climate and the Hadley circulation. Atmos Chem Phys 13:5227–5241
Trenberth KE (1997) The definition of El Niño. Bull Am Meteorol Soc 78:2771–2777
Trenberth KE, Jones PD et al (2007) Observations: surface and atmospheric climate change. In: Solomon S et al (eds) Climate change 2007: the physical science basis. Cambridge University Press, Cambridge, pp 235–336
Vecchi GA, Soden BJ (2007) Global warming and the weakening of the tropical circulation. J Clim 20:4316–4340
Washington R, James R, Pearce H, Pokam WM, Moufouma-Okia W (2013) Congo Basin rainfall climatology: can we believe the climate models? Phil Trans R Soc B 368:20120296
Williams AP, Funk C (2011) A westward extension of the warm pool leads to a westward extension of the Walker circulation, drying eastern Africa. Clim Dyn 37:2417–2435
Zhang R, Delworth TL (2006) Impact of Atlantic multidecadal oscillations on India/Sahel rainfall and Atlantic hurricanes. Geophys Res Lett 33, L17712